NMR RELAXATION STUDIES OF ALKALI METAL ION INTERACTIONS WITH THE GRAMICIDIN A TRANSMEMBRANE CHANNEL

Dan W. Urry

Laboratory of Molecular Biophysics
School of Medicine
University of Alabama at Birmingham
P. O. Box 311
Birmingham, AL 35294

Contents

I. Introduction

The magnitude of alkali metal ion currents that pass through the gramicidin A transmembrane channel in accessible ranges of ion activities and common applied potentials are in the approximate range of $10^{6.5}$ to 10^{8} ions/s (1-5). This is the range also found for channels from higher organisms (6). With the low voltage dependence of the off-rate constant for gramicidin A channels, in the absence of an applied potential (that is, under convenient circumstances for most NMR studies) and particularly at high ion concentrations, the off-rate constants would also be in the range of $10^{6.5}$ to 10^{8}/s. For those favorable cases where it can be demonstrated that the reciprocal of the ion correlation times, τ_c^{-1}, is dominated by the off-rate constant, k_{off} (7,8), this means that an optimal NMR observation frequency, ν_0, for the determination of the off-rate constant would also be in the $10^{6.5}$ to 10^{8} Hz range. More specifically for the alkali metal ions it appears that τ_c can be determined for spin 3/2 nuclei when $1.5 \leq (1+\omega^2\tau_c^2) \lesssim 200$

where $\omega = 2\pi\nu_0$. These are just the observation frequencies for which studies of the alkali metal ions can be carried out with commercially available NMR spectrometers.

While each alkali metal ion presents different issues to be considered, the casual perspective that the small electric quadrupole moment, for example, of ^{133}Cs (0.003 as opposed to 0.14 for ^{23}Na) would preclude effective use of this nucleus for relaxation studies is not borne out by the experimental results. This is most likely primarily due to the electric field gradient enhancing effect of the Sternheimer antishielding factor (9). As will be reviewed below, NMR relaxation studies of each of the alkali metal ions (^{7}Li, ^{23}Na, ^{39}K, ^{87}Rb and ^{133}Cs) allow estimates of binding constants. The spin 3/2 nuclei (^{23}Na, ^{39}K and ^{87}Rb), allow for reasonable estimates of ion correlation times when interpreted as ion occupancy times, τ_b, with $\tau_b^{-1} = k_{off}$. The ion binding constants determined at high ion concentration and the occupancy times also determined at high ion concentrations can be used to calculate reasonable currents and conductance ratios for the three ions (10). Studies on ^{7}Li (spin 3/2) result in the least effective calculation of currents but even these values can be used to calculate currents that are within a factor of two or three of the experimental currents (11). Of particular interest is spin 7/2 ^{133}Cs. On interaction with the gramicidin A transmembrane channel this ion exhibits two phenomenological components in the transverse relaxation which, when analyzed with the spin 3/2 formalism of Bull, yield correct ion occupancy times (12). The assessment of correct occupancy times is due to the capacity to calculate correctly the single channel currents over a wide concentration range, and it is due to the observation that at high ion activities the ion occupancy time and binding constant are essentially the same for spin 7/2 ^{133}Cs as for spin 3/2 ^{87}Rb. This is as required since Rb^+ and Cs^+ exhibit similar magnitudes of single channel currents (2-4,13,14). Thus an emerging aspect of using NMR relaxation methods for the study of ion interactions with the gramicidin A transmembrane channel is not only the advancement of our understanding of channel transport but also the demonstration of the efficacy of relaxation studies on each of the alkali metal ions.

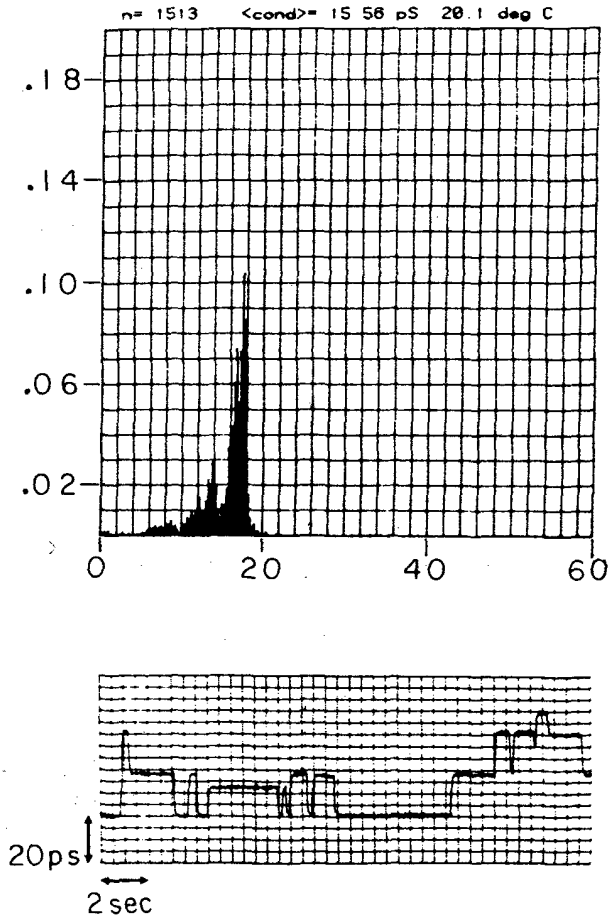

Figure 1. Lower part: Single channel conductance trace of HPLC purified Gramicidin A in a diphytanoyl phosphatidylcholine/n-decane membrane at 20° C, 100 mV for 1 M KCl. A step up is the "turning on" of a single channel and a step down is the "turning off" of a single transmembrane channel formed from two Gramicidin A molecules as shown in Figure 2. Upper part: Histogram of the frequency of occurrence of single channel conductance plotted as a function of the magnitude of the single channel conductance. The most probable single channel conductance, about 60% of all of the events, is between 16 and 18 pS (17 pS ± 1.5 pS). At 100 mV this is a flow of just over 10^7 ions/s. Reproduced with permission from reference 16.

II. The Gramicidin A Transmembrane Channel: Phenomenology, Structure and Ion Binding Sites

A. Channel Transport Phenomenology

Before proceeding to the ion NMR studies it is helpful to have a clear picture of channel transport phenomenology, of channel structure, and of the location of ion binding sites within the channel. The approach to the characterization of channel transport phenomenology is due to the original contributions of Mueller and coworkers (15). A planar lipid bilayer (a black lipid membrane) is formed in a small hole separating two water-filled chambers; the planar lipid bilayer makes the resistance to charge movement between the two chambers quite high. When a single channel spans the lipid bilayer membrane, a current passes through the single transmembrane channel that is sufficiently large to result in readily measured current steps. On dividing the single channel current, i, in amperes (coulombs/s) by the applied potential in volts, the single channel conductance is obtained which is usually given in picosiemens (pS). The single channel conductance steps due to gramicidin A channels turning "on" and "off" for 1 M KCl, 20°C, 100 mV and diphytanoyl A histogram giving the frequency of occurrence of single channel conductance steps for over 1500 events is given in Figure 1A. The most probable conductance steps are 17 ± 1.5 pS which represent about 60% of the events. The distribution of conductance states rather than a single conductance level has been proposed to arise from different side chain distributions for the channel state even though there is no direct contact of permeant ion with side chain (17).

B. Channel Structure

There is now general agreement that the gramicidin A channel structure is as proposed in 1971 (18,19,20). The primary structure of gramicidin A is HCO - L·Val[1]-Gly[2]-L·Ala[3]-D·Leu[4]-L·Ala[5]-D·Val[6]-L·Trp[13] D·Leu[14]-L·Trp[15]-$NHCH_2CH_2OH$ (21,22).

L·Trp[13]-D·Leu[14]-L·Trp[15]-$NHCH_2CH_2OH$ (21,22). As depicted in Figure 2, two molecules of gramicidin A, each in a single stranded β-helix with 6.2 to 6.3 residues/turn associate head to head (formyl end to formyl end) by means of six intermolecular hydrogen bonds to form a continuous helical structure. Along the helix axis is a channel approximately 4Å in diameter and 26Å in length which contains a single file of water molecules. Since the lateral coordinating groups for an ion in the channel are the electronegative carbonyl oxygens of librated peptide moieties, the channel is selective for cations; and as the single lateral helical wall surrounded by lipid provides insufficient solvation for divalent cations but quite satisfactory solvation for monovalent cations, the channel is impermeable to multivalent cations but selective for monovalent cations with currents for example for one molar K^+ (see Figure 1) of 17 pS $\times$ 0.1 volt = 1.7 picoAmp or 1.7×10^{-12} coulombs $s^{-1}/1.6 \times 1^{-19}$coulombs $ion^{-1} = 10^7$ ions/s (23).

C. Location of Ion Binding Sites

By means of a series of gramicidin A syntheses in which one carbonyl carbon at a time was 90% carbon-13 enriched, it has been possible to incorporate the channel state of synthetic singly carbonyl carbon labelled gramicidin A into a suspension of lipid bilayers and to use carbon-13 nuclear magnetic resonance to monitor the single carbonyl and to look for ion induced carbonyl carbon chemical shifts. In Figure 3 are the experimental ion induced carbonyl carbon chemical shifts plotted as a function of the location of the carbonyl in the channel structure for sodium ion and for thallium ion (24,25). A pair of localized, symmetry-related binding sites are observed just inside each entrance to the channel. In the following NMR relaxation studies, the difference between longitudinal and transverse relaxation rates for ions in aqueous suspension of lipid (i.e. in the absence of channels) and in the presence of channels in the lipid are used to obtain binding and rate constants. The sites responsible for the very substantial increases in relaxation rates on addition of channels are depicted in Figure 3. The lipid used was lysophosphatidyl-choline which on appropriate heat incubation with gramicidin A converts to lipid bilayers containing the channel state (26).

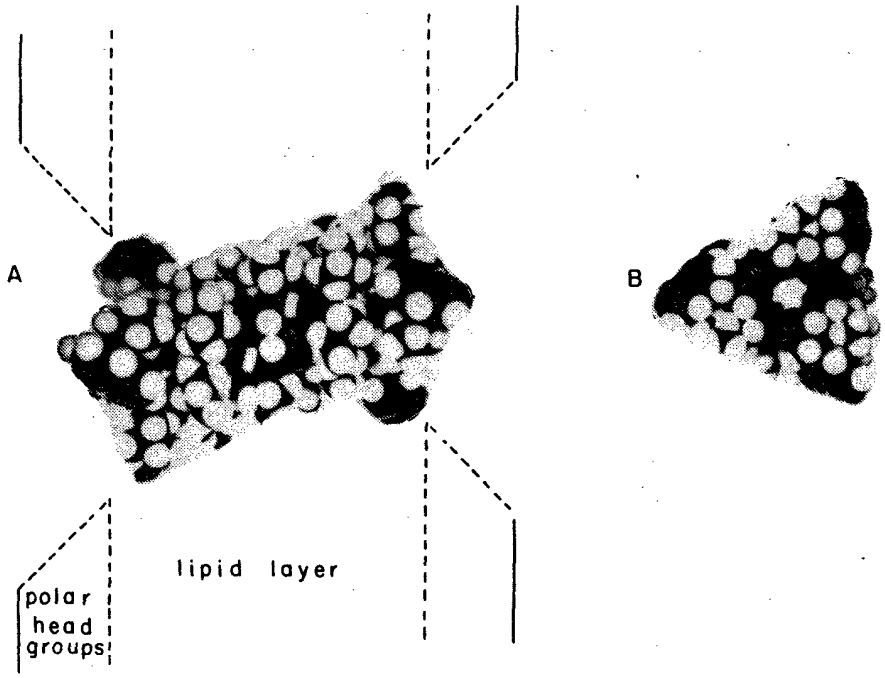

Figure 2 A. Space filling model of the Gramicidin A transmembrane channel schematically shown spanning the lipid layer of a lipid bilayer membrane. B. End view showing the channel through which monovalent cations can pass from one side to the other of the lipid bilayer membrane. It is through this channel that ions pass at currents of 10^7 ions/s or more.

III. Estimating Binding Constants using Longitudinal Relaxation Data

A. Excess Longitudinal Relaxation Rate Plots

Under conditions of fast exchange between aqueous solution and a binding site, the experimental longitudinal relaxation rate, $R_1 = 1/T_1$ where T_1 is the longitudinal relaxation time, is given by

$$R_1 = P_f R_{1f} + P_b R_{1b} \qquad (1)$$

where P_f and P_b are the mole fractions of ions free in solution and at a binding site, and $R_{1f} = 1/T_{1f}$ and $R_{1b} = 1/T_{1b}$ are the relaxation rates and times for the ion when free in solution and when bound. Since $P_f + P_b = 1$, the excess longitudinal relaxation rate, $(R_1 - R_{1f})$, that is the change in relaxation rates due to the addition of binding sites, becomes

$$(R_1 - R_{1f}) = P_b(R_{1b} - R_{1f}) \qquad (2)$$

With the total concentration of binding sites indicated as C_T and for the case where the unoccupied binding site concentration is negligible with respect to the total ion concentration, Me_T, James and Noggle (27) derived the expression

$$(R_1 - R_{1f})^{-1} = \frac{Me_T + K_b^{-1}}{C_T(R_{1b} - R_{1f})} \qquad (3)$$

For a single binding site a plot of $(R_1 - R_{1f})^{-1}$ versus Me_T gives a straight line. Since $(R_1 - R_{1f})^{-1} = 0$, $-Me_T = K_b^{-1}$, that is, the negative x-axis intercept obtained from the extrapolated straight line gives the reciprocal of the binding constant, K_b^{-1}.

For the gramicidin A transmembrane channel, as shown in Figure 3, there are two structurally identical binding sites. But due to repulsion between ions when there are two ions in the channel (double occupancy), the binding constant for achieving double occupancy, i.e. for the binding of the second ion, is weaker than the binding constant for entry of the first ion in the channel (single occupancy). The binding process for entry of the first ion is characterized by the tight binding constant, K_b^t and the process for entry of the second ion in the channel is characterized by the weak binding constant, K_b^w. As shown in Figure 4A for the interaction of sodium

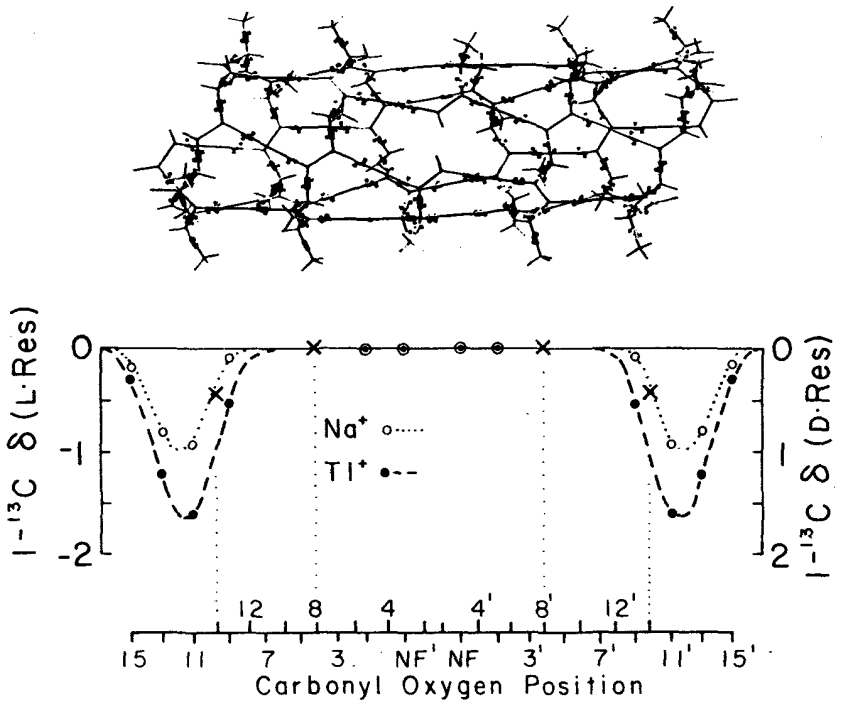

Figure 3. Upper part: Wire model of Gramicidin A transmembrane channel showing backbone atoms, β-carbons and hydrogen bonding between turns within each monomer and between monomers at the head to head (formyl end to formyl end). Lower part: Plots of ion induced carbonyl carbon chemical shifts for sodium ion (o) and for thallium ion (•). The observation of the ion induced carbonyl carbon chemical shifts determines the location of the ion binding sites just inside each mouth of the channel. Adapted with permission from reference 25.

ion with the channel, the excess longitudinal relaxation rate (ELR) plot is distinctly non-linear (7). If only the high concentration (high ion activity) range were accessible, e.g, from 0.5 to 1.0 molal activity, a binding constant of $2.6/M$ would be obtained from the reciprocal of the negative x-axis intercept. If only the low ion activity range were measured, e.g. from 0.02 to 0.20 molal activity, then a binding constant of $30/M$ would have been obtained. These intercepts are taken as reasonable comparative values for the weak and tight binding constants (11).

Another ion for which complete titration curves are possible is ^{133}Cs. Even though this is a spin 7/2 nucleus, on the basis of theoretical analyses (28) it is generally appreciated that there is one sufficiently dominant longitudinal relaxation component so that the James-Noggle analysis, initially considered appropriate to spin 3/2 nuclei, can be utilized for spin 5/2 and spin 7/2 nuclei. (As will be shown below for ^{133}Cs interaction with the gramicidin A channel, transverse relaxation data exhibit phenomenologically two components which, when treated like the two transverse relaxation components apparent under similar conditions for spin 3/2 nuclei, yield quite appropriate ion correlation times.) The excess longitudinal relaxation rate data as a function of cesium ion activity is given in Figure 4B (29). The limiting slope at high molal activities gives a negative x-axis intercept indicating a weak binding constant, K_b^w of $4.2/M$ while the slope at low ion activity indicates a tight binding constant, K_b^t of $60/M$.

B. Explicit Consideration of the Complete Expression for the Experimental Longitudinal Relaxation Rate

The excess longitudinal relaxation rate values plotted in Figure 4 for a given ion activity are calculated with respect to the longitudinal relaxation rate in the system of water plus phospholipid at the same ion activity. This is quite satisfactory for sodium and for cesium ions as their interaction with the

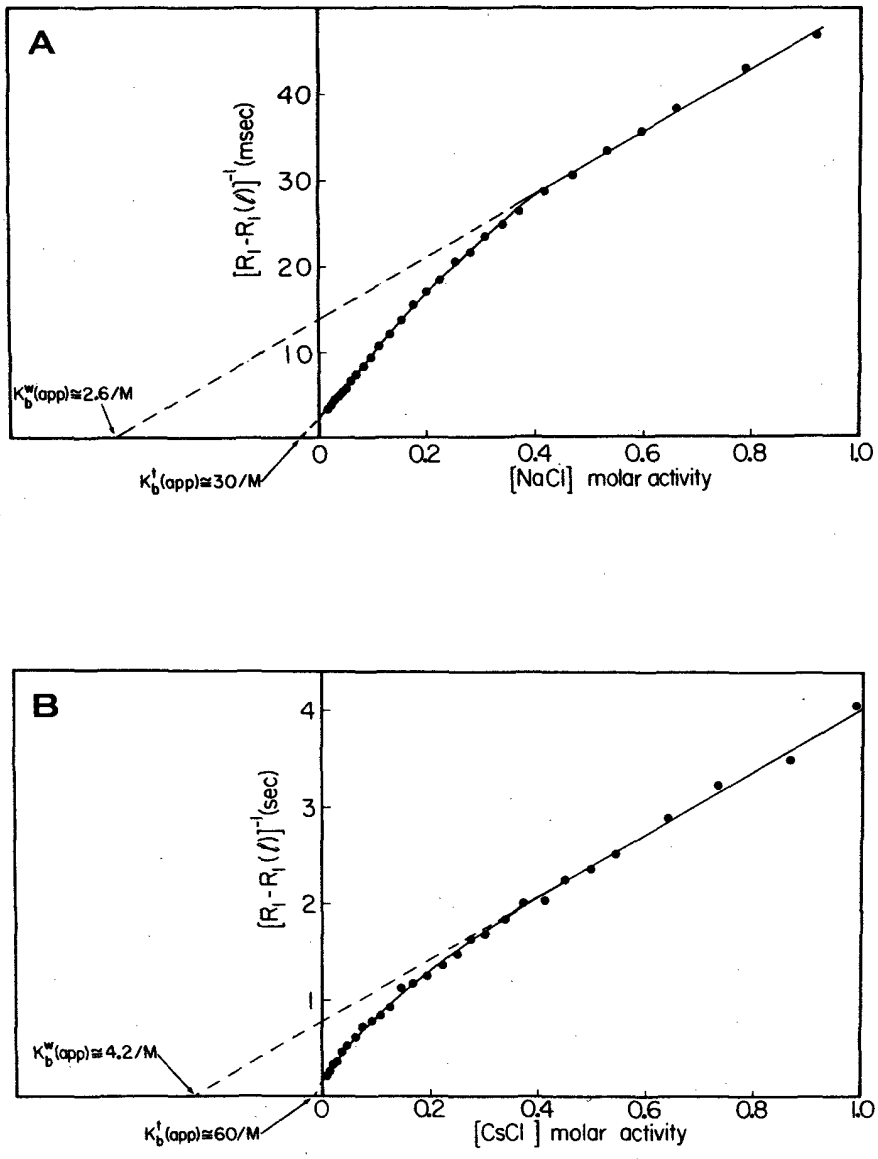

Figure 4 A. Excess longitudinal relaxation rate (ELR) plot for ^{23}Na ion interaction with 3 mM channels. The reciprocals of the negative x-axis intercepts for the low and high molal activity limits provide estimates for the tight, K_b^t and weak, K_b^w, binding constants, respectively. The values are 30/M and 2.6/M. Adapted with permission from reference 7. B. ELR plot for ^{133}Cs ion interaction with 3 mM channels. The binding constants are estimated to be $K_b^t \simeq 60$/M and $K_b^w \simeq 4.2$/M. Adapted with permission from reference 29.

phospholipid without channels is relatively weak. It is important, however, to consider the complete expression for the experimental longitudinal relaxation rate

$$R_1 = P_f R_{1f} + P_\ell R_1(\ell) + P_t R_{1t} + P_w R_{1w} \qquad (4)$$

where P_ℓ, P_t and P_w are the mole fraction of ions bound to phospholipid, to channel tight site and to channel weak site, respectively, and $R_1(\ell)$, R_{1t} and R_{1w} are the corresponding relaxation rates at the above noted sites (30). For 0.5 molal activity ion chloride the approximate longitudinal relaxation rates in water, in water plus phospholipid, and in water plus phospholipid plus channel are, respectively, 0.027/s, 0.056/s and 0.089/s for ^{7}Li; 0.019/ms, 0.021/ms and 0.067/ms for ^{23}Na; and 0.087/s, 0.102/s and 0.704/sec for ^{133}Cs The factors by which the longitudinal relaxation rates increase

on going from water to water plus phospholipid and from water plus phospholipid to water plus phospholipid plus channels, respectively, are 2.07 and 1.6 for ^{7}Li, 1.1 and 3.2 for ^{23}Na, and 1.15 and 6.9 for ^{133}Cs. The larger the factor on addition of channels, particularly when compared to the factor for going from water to water plus phospholipid, the more favorable the data for analysis in terms of binding constants. The data for ^{133}Cs are clearly the most favorable in spite of its small electric quadrupole moment and the data for ^{7}Li are clearly the least favorable.

By considering stepwise the increasing complexity of the system, i.e., by first analyzing the change in longitudinal relaxation time on addition of phospholipid ($R_1 = P_f R_{1f} + P_\ell R_1(\ell)$) and solving for P_f, P_ℓ and $R_1(\ell)$), and then by adding the channel in the phospholipid, it is possible to fit the data in Figure 4 to determine P_t, R_{1t}, P_w and R_{1w}. The binding constants, of course, are obtained from P_t and P_w along with P_f and P_ℓ, and R_{1t} and R_{1w} are found to be different. In general $R_{1w} > R_{1t}$ by a factor of two or three, presumably due to the contribution on double occupancy of one ion to the electric field gradient of the other ion. While the complete fit may give the best values of K_b^t and K_b^w for a given set of data there is not a well-defined local minimum in the fit to the data due to the four parameters required. Because the variation in values for R_{1t} and R_{1w} can arise from subtle variations in the titration, comparisons between data on different ions have this added uncertainty. For each of the ions the complete expressions have been used; for comparison between ions, however, it was considered most reliable to use the James-Noggle intercept approach which for multiple binding processes does not explicitly contain the differences in relaxation rates at the different sites (11). The values so obtained are given in Table I (7,8,10,29,30).

Table I. Binding Constants for Alkali Metal Ion Interactions with the Gramicidin A Transmembrane Channel.

Ion	K_b^t	K_b^w	Reference
^{7}Li	25/M	0.77/M	(30)
$^{23}Na^+$	30/M	2.6/M	(7)
$^{33}K^+$	~50/M[a]	8.3/M	(10)
$^{87}Rb^+$	(~60/M)[b]	3.9/M	(8)
$^{133}Cs^+$	60/M	4.2/M	(29)

[a]The estimate of K_b^t for K^+ was not obtained from ELR data but rather was estimated from the concentration dependence of Trp[11] carbonyl carbon chemical shifts.
[b]The estimate of K_b^t for Rb^+ was not obtained from ELR data but was taken to be the same as for Cs^+ as both these ions have similar values for K_b^w.

IV. Estimating Ion Correlation Times Using Transverse (and Longitudinal) Relaxation Data

A. Four Experimental Cases of Observable Lineshapes for Alkali Metal Ions

The experimentally observable lineshapes and the differing analyses of the results required to determine rate constant data may be considered according to the magnitude of $\omega^2\tau_c^2$. There are four experimental cases to delineate (see the Figure 5).

The reality, of course, is a continuous spectrum of possible results beginning with the extreme narrowing condition ($\omega^2\tau_c^2 << 1$) and progressing to situations where $\omega^2\tau_c^2$ is as large as several hundred. The study of alkali metal ion interactions with the gramicidin A transmembrane channel involves consideration of each of the four cases, and for three of the four cases the magnitude of rate constants relative to channel transport can be obtained. *Case 1 The Lorentzian Line Shape*

The Lorentzian line shape can be characterized by the ratio of the total line width at one-eighth of the total peak height to the total line width at one-half of the peak height i.e. $\nu_{1/8}/\nu_{1/2} = \sqrt{7} = 2.65$. The situation that generally gives rise to a Lorentzian lineshape is the extreme narrowing condition where $\omega^2\tau_c^2 << 1$. This situation is further verified by demonstrating that $T_1 = T_2$, i.e.,

$$\frac{1}{T_1} = \frac{1}{T_2} = \frac{\chi^2}{10}\tau_c \qquad (5)$$

and by demonstrating that T_1 and T_2 are independent of magnetic field strength, that is independent of observation frequency, $\nu_0 = \omega/2\pi$. In the case of ^{23}Na with a 23.5 kG field, $\tau_c << 6\times 10^{-9}$ s. This case obtains for all of the alkali metal ion chlorides

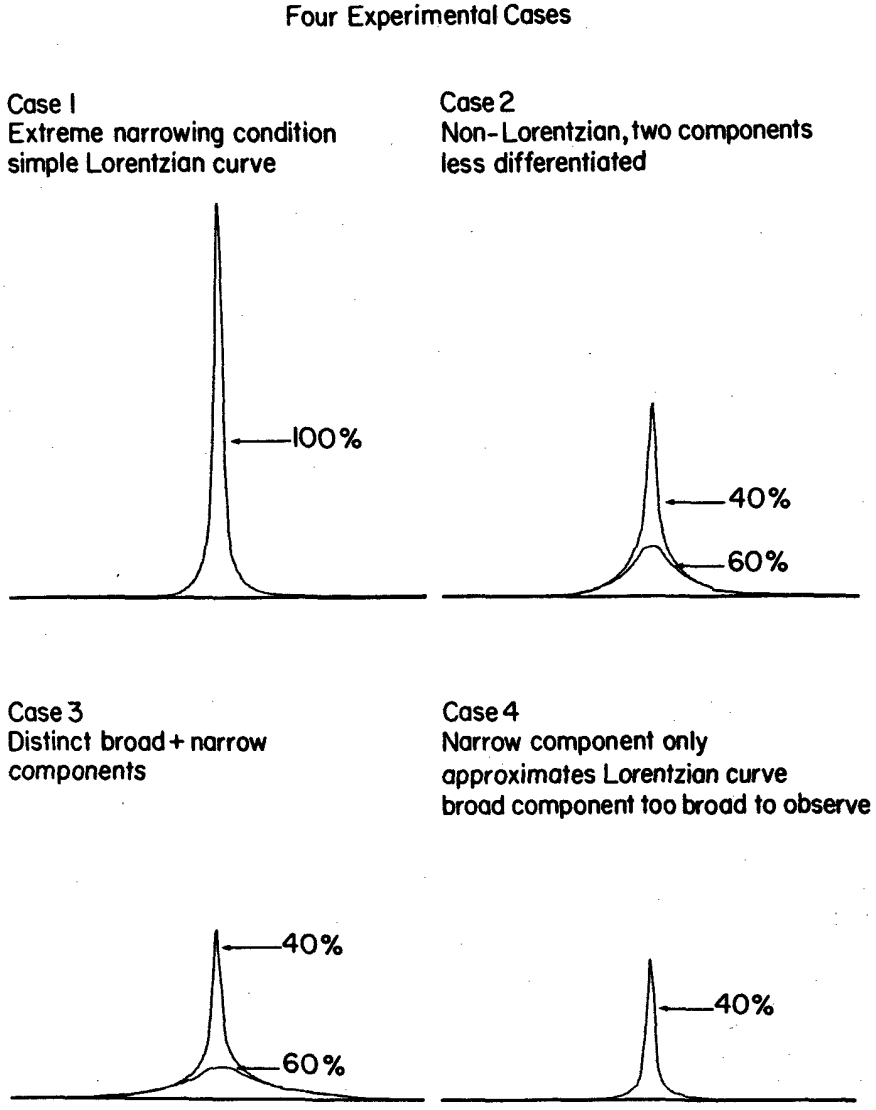

Figure 5. Four experimental classes of resonance lines obtained when quadrupolar nuclei interact with binding sites under conditions of rapid exchange. In each case the analysis of the transverse relaxation process can proceed differently. See text for detailed discussion. Adapted with permission from reference 11.

in water. Fortunately it does not obtain in the presence of channels as the magnitude of the quadrupolar coupling constant, χ, would have to be known in this case before the magnitude of τ_c could be determined.

Case 2 A Non-Lorentzian Line Shape (but not clearly multiple Lorentzian)

This case occurs when $\omega^2\tau_c^2 \simeq 1$. T_1 is found to differ from T_2 and the $\nu_{1/8}/\nu_{1/2}$ ratio is found to be greater than $\sqrt{7}$. Using the formalism of Bull (31), Rose and Bryant (32) presented an approximate expression for the ratio of the excess transverse relaxation rate, ΔR_2 to the excess longitudinal relaxation rate, ΔR_2 i.e.,

$$\frac{\Delta R_2}{\Delta R_1} = \frac{R_2 - R_{2f}}{R_1 - R_{1f}} \tag{6}$$

$$= \frac{0.6 + 0.4(1 + 4\omega^2\tau_c^2)^{-1} + (1 + \omega^2\tau_c^2)^{-1}}{1.6(1 + 4\omega^2\tau_c^2)^{-1} + 0.4(1 + \omega^2\tau_c^2)^{-1}} \tag{7}$$

Of course the inverse of the transverse relaxation time, $1/T_2$, is the experimental transverse relaxation rate in the presence of channels, R_2, and R_{2f} is the transverse relaxation rate for the ion free in solution or for the chosen reference state which for

our cases will be in the presence of lipid $R_2(\ell)$ but in the absence of channels.

Potassium-39 An example of this case is shown in Figure 6 (10); it results from the interaction of 1 M K^+ with 0.3 mM channels at 30° C and an observation frequency of 4.65 MHz. With $T_1 = 15.3$ ms, $T_2 = 7.3$ ms, $T_1(\ell) = 55$ ms and $T_2(\ell) = 50$ ms, the value of $\Delta R_2/\ \Delta R_1$ is 2.48. By eqn. 7, plotted in Figure 7B, the value of the ion correlation time, τ_c, is 3.89×10^{-8} s. With the observation frequency for ^{39}K of 4.65×10^6 Hz, the value of $\omega^2\tau_c^2$ would be 1.29, i.e., in the range of one. As will be seen below for ^{23}Na, the resonance for 1 M NaCl at 30° in the presence of 3 mM channels obviously comprises two components, yet the ion correlation time is 4.8×10^{-8} s, only 20% greater than for the potassium case. The reason, therefore, that ^{39}K observation of 1 M KCl interaction with the channel is an example of Case 2 is the low observation frequency used for ^{39}K, being nearly one-sixth that used for ^{23}Na.

Case 3 Observation of Both Broad and Narrow Components

The observation of both broad and narrow components can occur when $\omega^2\tau_c^2$ is substantially larger than one. For the composite resonance line, of course, $\nu_{1/8}/\nu_{1/2}$ is significantly greater than $\sqrt{7}$, and T_1 is found to be larger than T_2. Each substituent component, however, is found to be well represented by a Lorentzian function. As shown by Bull (31), the decay of the transverse magnetization, M_T, is given for spin 3/2 nuclei by

$$M_T(t) = M_T(0)[0.6exp(-\tau/T_2') + 0.4exp(-\tau/T_2'')] \quad (8)$$

where T_2'' is the relaxation time of the broad (fast) component and T_2' is that of the narrow (slow) component, and the corresponding transverse relaxation times are R_2' and R_2''. An expression for the very useful ratio of the excess transverse relaxation rates, $\Delta R_2'$, and $\Delta R_2''$, due to Bull (31) is

$$\frac{\Delta R_2'}{\Delta R_2''} = \frac{R_2' - R_{2f}}{R_2' - R_{2f}}$$

$$= \frac{1 + (1 + \omega^2\tau_c^2)^{-1}}{1 + 4\omega^2\tau_c^2)^{-1} + (1 + \omega^2\tau_c^2)^{-1}} \quad (9)$$

where R_{2f}, is the transverse relaxation rate for the reference state which is commonly the ion in an aqueous solution. The conditions for which eqn. (9) and eqn. (7) are applicable are: 1) for rapid exchange between two sites where one site is represented by the extreme narrowing condition (e.g. an ion free in solution) and the second site is not under the extreme narrowing condition (i.e. the binding site), 2) for the occupancy time of the ion in the site which is shorter than the relaxation time of the ion bound in the site, and 3) for a situation where the mole fraction of free ion, P_f, is sufficiently greater than that of the bound ions, P_b, that P_f may be taken as one. For the applications demonstrated here the reference state is taken as the transverse relaxation rate of the same concentration of ion in an aqueous solution plus lipid, $R_2(\ell)$, such that the excess transverse relaxation rate of interest is that due to the addition of channels, that is, the situation for ion in the aqueous solution plus lipid is sufficiently close to the extreme narrowing condition for that assumption to be used.

There are three means of measuring T_2' and T_2'' when two components are reasonably discernible. They are 1) curve resolution, 2) the null method and 3) the spin echo method. Each approach is represented below by an alkali metal ion. Curve resolution is exemplified by ^{23}Na data, the null method by ^{87}Rb data and the spin echo method by ^{133}Cs and ^{7}Li data.

a. Sodium-23 The resonance line obtained for 1 M NaCl at 30° in the presence of 3 mM channels is given in Figure 8A (7) and the resolution into a broad component with 60% of the total intensity (area) and a narrow component with 40% of the total intensity. This is in accordance with eqn. (8). The full line width at half intensity for the broad component, $\nu_{1/2}$, is 325 Hz giving a value for $R_2' = (\pi\nu_{1/2}')$ of 1.02×10^3/s. The full line width at half intensity for the narrow component, $\nu_{1/2}''$, is 16 Hz giving a value for R_2'' $(=\pi\nu_{1/2}'')$ of 50.3 s. The relaxation rate in the presence of lipid but the absence of channels, $R_2(\ell)$, is 31.4/s. By eqn. (9) the ratio would be 52.3 and the sodium ion correlation time would be 4.8×10^{-8} s (33-35). With an observation frequency for ^{23}Na of 26.4×10^6 Hz the value of $\omega^2\tau_c^2$ would be 63, i.e., substantially greater than one.

b. Rubidium-87 A stack of spectra using the 180° - τ - 90° pulse sequence is given in Figure 9 for 2 M RbCl at 30° in the presence of 3.16 mM channels (8). The τ values were chosen in order to null one component and leave the other component from which a line width can be determined. With this

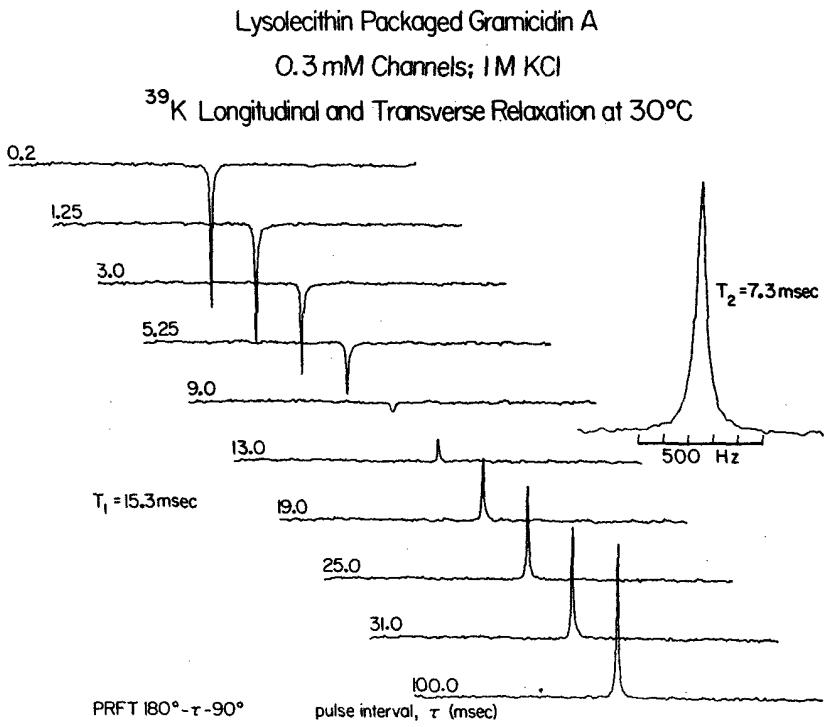

Figure 6. Longitudinal and transverse relaxation data for ^{39}K ion interaction (1 M KCl) with 0.3 mM Gramicidin A channels. This data is analyzed by eqn. (7), perhaps with the aid of Figure 7B, to determine the ion correlation time. This is an example of *Case 2* of Figure 5. Reproduced with permission from reference 10.

method both the longitudinal and transverse relaxation times can be obtained for each component as $T_1 = \tau_{null}/0.69$. It is interesting to note that the difference in T_1' and T_1'' is only 15% whereas there is a 500% difference in T_2' and T_2''. This makes the latter data very useful in estimating an ion correlation time. With $R_2' = 6.62 \times 10^3$/s and $R_2'' = 1.33 \times 10^3$/s, as obtained from Figure 9, and with $R_2(\ell) = 526$/s, the ratio of the excess transverse relaxation rates for the two components becomes 7.6. By eqn. (9) or using the plot of this equation in Figure 7A, this ratio gives a value for τ_c of 1.35 x 10^{-8} s. With an observation frequency of 32.6×10^{-8} Hz for ^{87}Rb $\omega^2\tau_c^2$ would be 7.6. This is greater than one and the same magnitude as the ratio itself.

c. Cesium-133 Even though ^{133}Cs is a spin 7/2 rather than a spin 3/2 nucleus, phenomenologically on interaction with the gramicidin A transmembrane channel two components are observed in the ^{133}Cs resonance, just as occurs for the spin 3/2 nuclei. Furthermore it will be shown below that the inverse of the ion correlation time is the off-rate constant and that the off-rate constant at high ion concentration and the weak binding constant (determined above) are sufficient to calculate the single channel currents at high ion concentration for Na^+ K^+ and Rb^+. It becomes possible, therefore, to see if eqn. (9) can be used for ^{133}Cs data to obtain an approximately correct value for the ion correlation time. If a reasonable value for the cesium ion single channel current can be obtained using eqn.(9), then it must be giving approximately correct values of τ_c for spin 7/2 ^{133}Cs. Data for ^{133}Cs is given in Figure 10 (12). Using the spin echo approach with a Carr-Purcell-Meiboom-Gill pulse sequence, at 30 mM CsCl a plot of the log of the transverse magnetization versus time shows two relaxation processes, a fast process with a characteristic time of $T_2' = 1.2$ ms and a slow process with a T_2'' of 23 ms. Similarly at high concentration, 1.5 M CsCl, two components are observed with $T_2' = 98$ ms and $T_2'' = 286$ ms. Additionally as may be seen in Figure 11

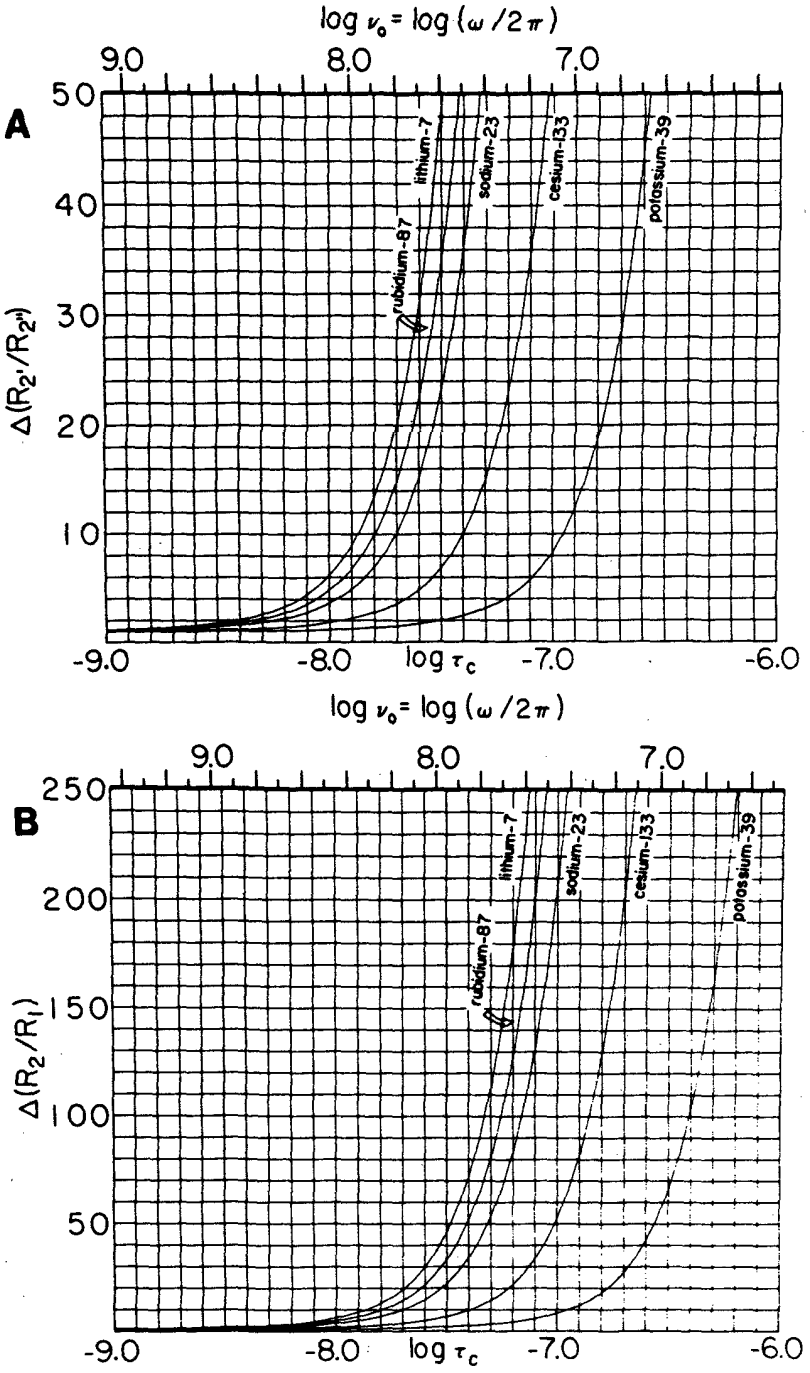

Figure 7 A. Plot of eqn. (9) for each of the alkali metal ions for a 23.5 kG magnetic field. The observation frequency is given as the abscissa at the top of the graph. For any desired frequency simply translate the curve horizontally to the desired frequency as read at the top of the graph. B. Plot of eqn. (7) for each of the alkali metal ions. Reproduced with permission from reference (11).

(29) using the null approach for 210 mM CsCl, two dominant components are observed. A third narrow line is observed but its intensity is so small as not to contribute significantly to the transverse magnetization. With $T_{2f} = T_2(\ell) = 5$ s the ratios of the excess transverse relaxation rates for 30 mM, 210 mM and 1.5 M CsCl are 19.2, 12, and 2.76, respectively. The value of 12 for the ratio from Figure 11 is simply

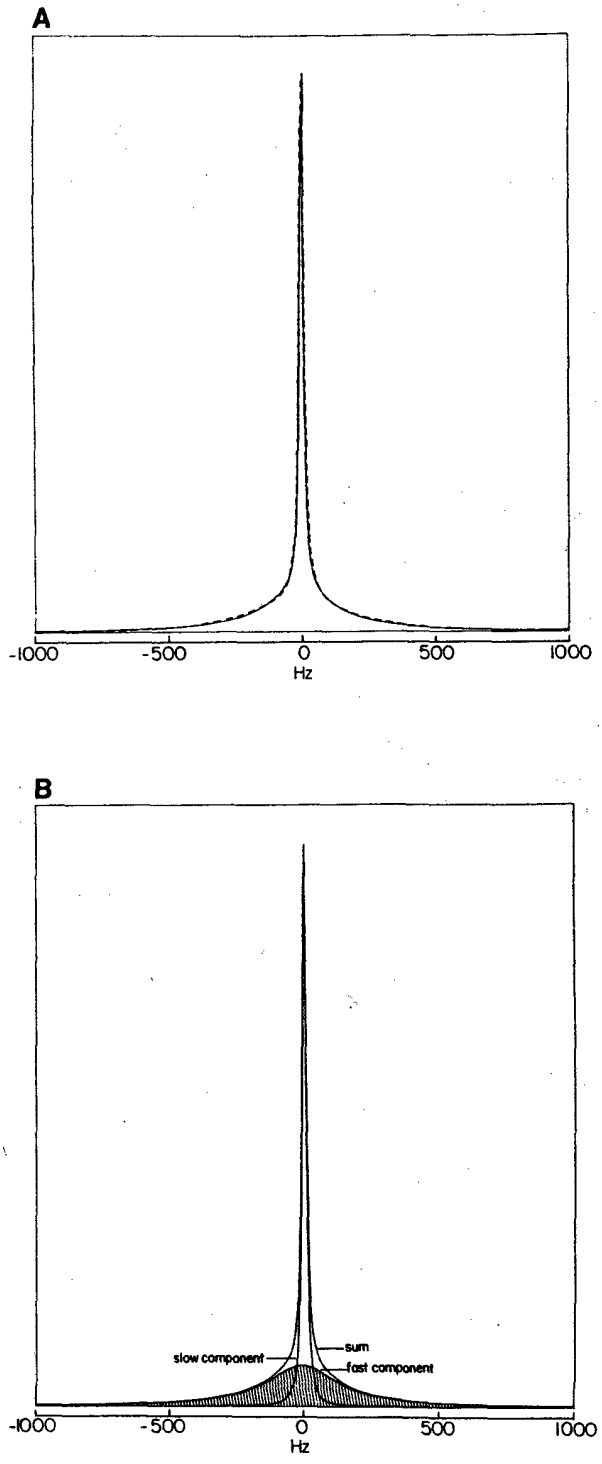

Figure 8 A. ^{23}Na resonance line for 1 M NaCl at 30° in the presence of 3 mM channels which is comprised of both narrow and broad Lorentzian components. The solid curve is the experimental curve and the dashed curve is the sum of the resolved narrow and broad components shown in B. The ratio of areas of the broad to narrow components is 60/40 in accordance with eqn. (8). $R_2' = \pi\nu_{1/2}' = 1021/s$ and $R_2'' = \pi\nu_{1/2}'' = 50.3/s$. These values by eqn. (9) and a value for $R_{2f} = R_2(\ell)$ of 31.4/s result in a τ_c of 48 ns.

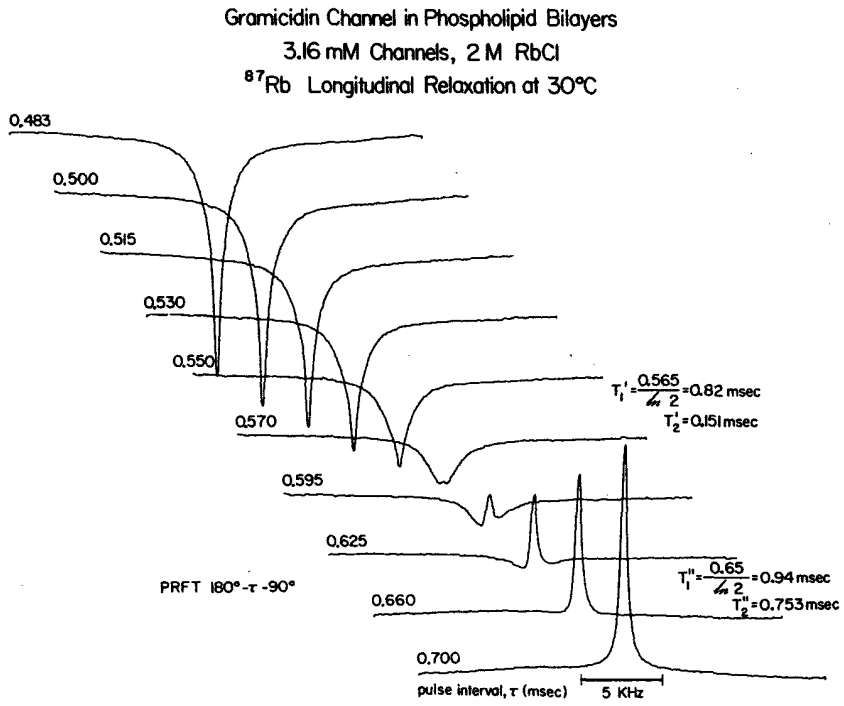

Figure 9. A stack of inversion-recovery (180° - τ - 90°) spectra for ^{87}Rb (2 M RbCl) in the presence of 3.16 mM channels. At the null for the narrow and then the broad component the line width at half intensity can be determined for the remaining component. $R_2' = \pi\nu_{1/2}' = 6.6$/ms and $R_2'' = \pi\nu_{1/2}'' = 1.33$ ms. With $R_2(\ell) = 526$/s, a value of τ_c is calculated by eqn. (9) to be 1.35×10^{-8} s.

the ratio of the line width of the broad component divided by the line width of the narrow component, i.e., $\nu_{1/2}'/\nu_{1/2}''$. In sequence the τ_c values would be 5.7×10^{-8} s, 4.5×10^{-8} s and 1.69×10^{-8} s. The intermediate value obtained for 210 mM CsCl would be due to contributions from a mixture of singly and doubly occupied channel states (note the binding constants determined above), whereas the 30 mM data would more nearly represent the singly occupied state and the 1.5 M data the doubly occupied state. The values of $\omega^2\tau_c^2$ for 30 mM, 210 mM and 1.5 M CsCl are 21.8, 13.6 and 1.9, respectively. As is apparent from Figure 10 on raising the concentration to 1.5 M CsCl, the fast component has become closer in magnitude to the slow component. (With the small value of $\omega^2\tau_c^2$ for 1.5 M CsCl one could wonder whether *Case 2* might not be also applicable. In this regard it should be appreciated that eqn.(7) depends on the approximation that $R_1 = 0.6R_2' + 0.4R_2''$. As is apparent from the intercept of Figure 10B, the two phenomenological components do not compare in intensity with a 60/40 ratio and therefore eqn.(7) is not applicable.) It will be shown below that the 1.5 M data is sufficient to calculate reasonable currents at high ion concentrations and in fact, the τ_c values at low and at high ion concentrations can be used to calculate reasonable currents over the entire concentration range (12).

d. Lithium-7 Among the alkali metal ion nuclei considered here as suitable for characterizing ion transport through the GA channel, the ^{7}Li nucleus is the least favorable. This is the situation for two major reasons: Firstly the small electric quadrupole moment, Q, and the smallest Sternheimer antishielding factor (9,36,37), γ_∞. (see Table II) mean that the quadrupolar relaxation mechanism, which would be proportional to $Q(1 - \gamma_\infty)$, may only be one of the mechanisms contributing to nuclear relaxation. Another important mechanism is likely dipole-dipole relaxation (38,39,40). Secondly of the alkali metal ion nuclei, ^{7}Li has the highest observation frequency, that is the largest gyromagnetic ratio. As may be seen in Figure 7 this means that it would be most suitable for Group 1 compara-

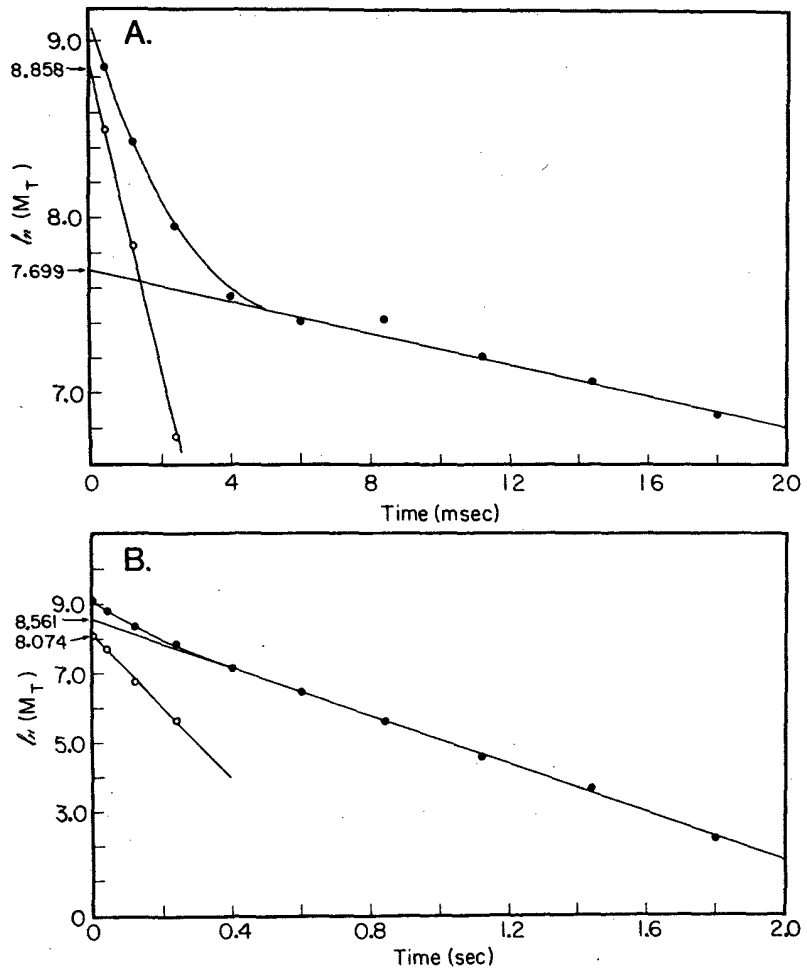

Figure 10. Decay of the transverse magnetization (spin echo experiment using the Carr-Purcell-Meiboom-Gill sequence) for 30 mM (part A) and 1.5 M CsCl (part B) in the presence of 3 mM channels. In both cases ln M_T is found to be comprised of two components. As discussed in the text, the two decay constants for this spin 7/2 nucleus can be used to calculate an ion correlation time using the formalism for spin 3/2 nuclei (eqn. 9) and the ion correlation time can be used to calculate single channel currents to the same degree of accuracy as for the spin 3/2 nuclei: ^{23}Na, ^{39}K and ^{87}Rb (10, 11, 12).

tive studies where the ion correlation time would be shorter than for the other ion. Considering the relationship demonstrated below as given in eqn.(18), this would be most favorable for situations where the off-rate constant for Li^+ would be larger than for the other alkali metal ions. For the GA channel the inverse is the case as the lithium ion single channel current is more than an order of magnitude smaller than that of Rb^+ and Cs^+, that is, lithium ion has the smallest off-rate constant of the alkali metal ions.

With these problems and limitations in mind it is yet of interest to see what the spin echo method would give for the ion correlation time when approximated using eqn.(9). The data are given in Figure 12 in the presence of 3 mM channels for 1 M LiCl; R_2, is 4.35/s and R_2'' is 0.25/s. With a value for $R_2(\ell)$ of 0.083/s the Bull ratio, $\Delta R_2,/\Delta R_2''$, becomes 25.6 which by Figure 7 or eqn.(9) gives an ion correlation time of 2.2×10^{-8} s. This differs by a factor of five (500%) from the value that would give the correct lithium ionic current and the correct ionic conductance ratios with respect to the other alkali metal ions. Initially it was thought that obtaining a calculated current using NMR-derived binding and rate constants, which was within a factor of ten (1000%) of the electrically measured current, would constitute a successful effort. Now for the spin 3/2 nuclei

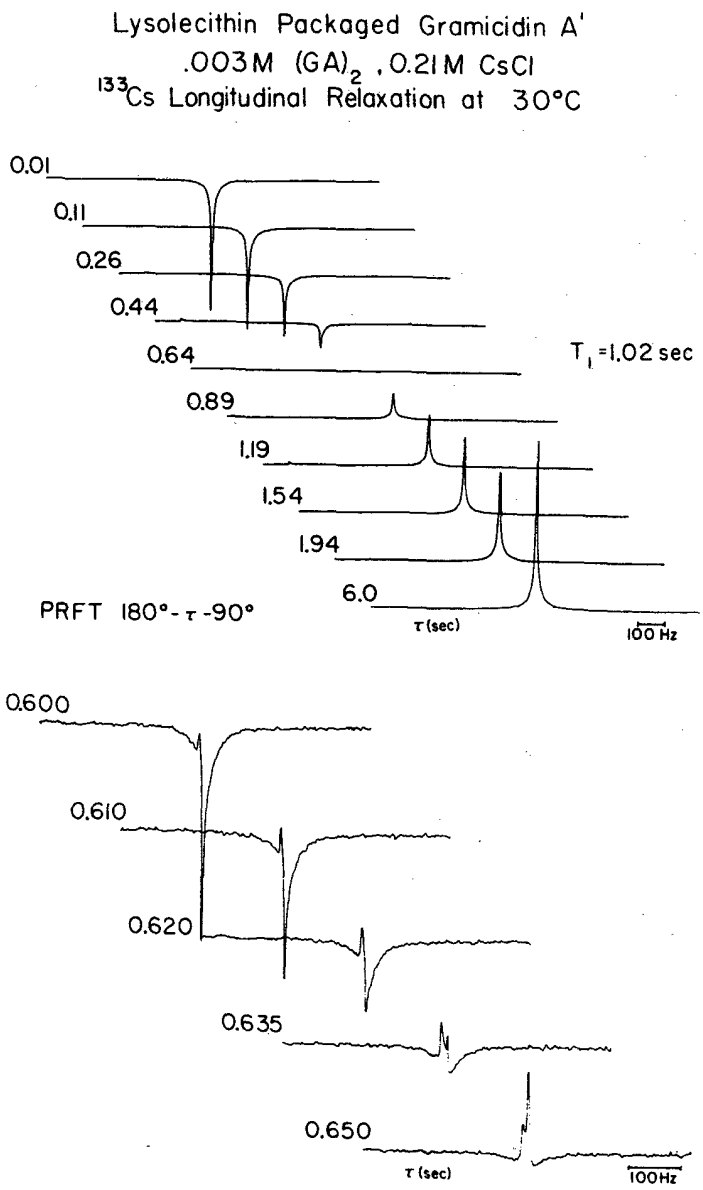

Figure 11. Partially relaxed Fourier transform data for ^{133}Cs using the inversion- recovery approach with 210 mM CsCl in the presence of 3 mM channels. By carefully examining the null region there is seen to be a single dominant intense narrow component and a broad component. A third narrow component is also observed, but it is of such low intensity that it would not contribute significantly to the data of Figure 10. Reproduced with permission from reference 29.

^{23}Na, ^{39}K and ^{87}Rb, it has been found that the error is closer to 10% (10,11). The success for these three alkali metal ions suggest a closer look at the ^{7}Li data with the consideration of including the dipole-dipole relaxation mechanism. Rewriting eqn.(1) for the transverse relaxation rate and including both the dipole-dipole (DD) and quadrupolar (Q) relaxation mechanisms gives

$$R_2 = P_f R_{2f} + P_b(R_{2b}(Q) + R_{2b}(DD)) \qquad (10)$$

Following Bull (31) and writing the ratio for the two components observed in the spin echo experiment (see Figure 12), the ratio in eqn.(9) becomes

$$\frac{\Delta R_2'}{\Delta R_2''} = \frac{R_2' - R_{2f} - P_b R_{2b}'(DD)}{R_2'' - R_{2f} - P_b R_{2b}''(DD)} \qquad (11)$$

with the ratio equalling the same expression as the right hand side of eqn.(9). As R_2', is so much larger than R_2'' which is itself greater than P_b R_{2b}''(DD), we consider only the narrow component R_{2b}''(DD) which

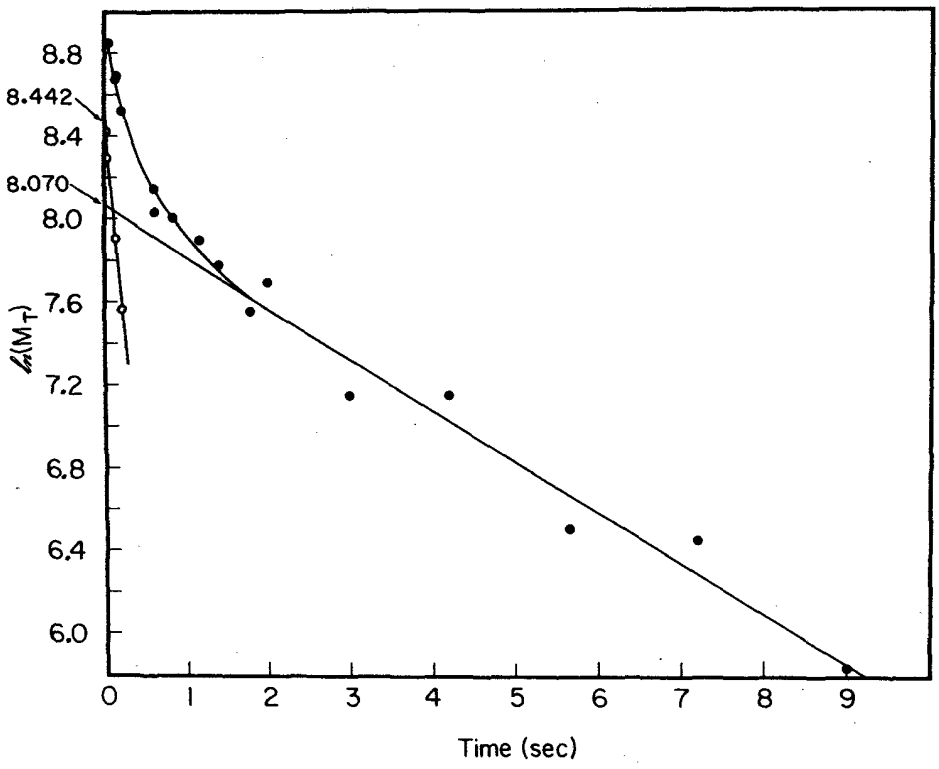

Figure 12. Spin echo (CPMG) experiment for 1 M LiCl in the presence of 3 mM channels. A fast and a slow process are observed with the relaxation rates $R_2' = 4.35/s$ and $R_2'' = 0.25/s$. The value for $R_2(\ell)$ is 0.083/s. These data are considered in terms of the quadrupolar relaxation mechanism using eqn. (9) and in terms of both quadrupolar and dipole-dipole relaxation mechanisms being operative using eqns. (11) and (12). See text for discussion. Reproduced with permission from reference 11.

concerns the spin $+1/2$ to $-1/2$ transition. Utilizing the formalism for spin 1/2 nuclei (41,42),

$$R''_{2b}(DD) = \frac{\hbar\gamma_H^2\gamma_{Li}^2}{20}\sum_j r_j^{-6}\left[\frac{\tau_c}{1+(\omega_H-\omega_{Li})^2\tau_c^2}\right.$$
$$+\frac{3\tau_c}{1+\omega_{Li}^2\tau_c^2}+\frac{6\tau_c}{1+(\omega_H+\omega_{Li})^2\tau_c^2}$$
$$\left.+\frac{6\tau_c}{1+\omega_H^2\tau_c^2}+4\tau_c\right] \qquad (12)$$

The molal activity of 1 M LiCl would be 0.78. With the binding constants of Table I the mole fraction of bound ions, P_b' would be 3.42×10^{-3} s and for τ_c to approximate the correct current, $R''_{2b}(DD)$ would be 47/s. In the case of eqn.(12) the fluctuation of the dipole-dipole interaction would be that due to the ion entering and leaving the channel. As before, taking the excess with respect to the system without channels, i.e. $R_2(\ell)$ replacing R_{2f}, and using a value of $2.34 \times 10^{46}/\text{cm}^6$ for $\sum_j r_j^{-6}$, the value of τ_c which simultaneously fits eqn.(12) and eqn.(9) with the ratio as defined in eqn.(11) becomes 1.18×10^{-7} s. This is by choice the number that will give the correct current; the question therefore is whether the distance for $\sum_j r_j^{-6}$ is reasonable. This distance would be equivalent to four hydrogen nuclei at a distance from the lithium nucleus of 2.4Å which is not unreasonable.

The ion correlation times as obtained above for each of the alkali metal ions are given in Table II.

Case 4 Near-Lorentzian Line Shape Because Broad Component too Broad to Observe

In this case the relaxation for the broad component is so fast that its relaxation has largely occurred during the delay time before the instrument begins accumulation of data. While $\nu_{1/8}/\nu_{1/2}$ may approximate $\sqrt{7}$, a major test for this situation is that the values of T_1 and T_2 are dependent on the magniture of the magnetic field, i.e. on observation

Table II. Ion Correlation Times for Alkali Metal Ion Interactions with the Gramicidin A Transmembrance Channel.

Ion	Electric quadrupole moment, Q	Sternheimer antishielding factor[b], γ_∞ as $(1-\gamma_\infty)$	$Q(1-\gamma_\infty)$	τ_c
$^{7}Li^{+}$	–0.03	0.74	0.022	2.2×10^{-8} s (1.18×10^{-7} s)[b]
$^{23}Na^{+}$	0.14–0.15	5.1	0.714	4.8×10^{-8} s
$^{39}K^{+}$	0.14	18.3	2.013	3.89×10^{-8} s
$^{87}Rb^{+}$	0.13	48.2	6.266	1.35×10^{-8} s
$^{133}Cs^{+}$	–0.003	111	0.333	1.69×10^{-8} s[c]

[a]The Sternheimer antishielding factor values are due to Schmidt et. al. (36).
[b]Obtained on introduction of the dipole-dipole relaxation mechanism for ^{7}Li with the τ_c chosen to give the correct off-rate constant (see eqn.18). The test for this is whether the distance dependence obtained for Li–H internuclear distances for the ion in the channel is reasonable. The value is equivalent to four hydrogen nuclei each at 2.4Å from the lithium nucleus. This is a reasonable value.
[c]Assuming that eqn. (9), which was derived for spin 3/2 nuclei (32), is applicable to ^{133}Cs which is a spin 7/2 nucleus.

frequency. This differentiates *Case 4* from *Case 1*. Another means is to integrate the signal and compare its intensity to that of a standard as shown in Figure 13 (11). For 20 mM NaCl the signal is integrated in the presence of lipid and this intensity is compared to that of 20 mM NaCl when channels have been added to the system. As seen in Figure 13, in the presence of channels only 40% of the intensity found for 20 mM NaCl is observed. This means that the ion correlation time is long, which would relate to a slow off-rate constant.

An attempt to estimate an exchange rate is possible if this remaining narrow component is treated as that of a spin 1/2 nucleus. For the case of rapid exchange in terms of chemical shift, ν.

$$\nu = P_f\nu_f + P_b\nu_b \qquad (13)$$

where ν_f and ν_b are the chemical shifts for the free and bound ion. It is convenient to take as the reference chemical shift that of the ion free in solution, i.e. $\nu_f = 0$, and P_b and ν_b can be determined from a titration of chemical shift versus ion concentration. In terms of line width one can write

$$\nu_{1/2} = \nu^f_{1/2} + P_b(\nu^b_{1/2} - \nu^f_{1/2}) + 4\pi P_b(1-P_b)^2\frac{\nu_b^2}{k_{off}} \qquad (14)$$

where $\nu^f_{1/2}$ and $\nu^b_{1/2}$ are the line widths for the free ion and the bound ion. The latter is obtainable from fitting the data in a linewidth versus ion concentration plot. Combining eqns. (10) and (11) gives

$$\nu_{1/2} = \nu^f_{1/2} + \frac{\nu}{\nu_b}(\nu^b_{1/2} - \nu^f_{1/2}) + \frac{4\pi(\nu_b-\nu)^2}{\nu_b k_{off}} \qquad (15)$$

Thus a plot of $\nu_{1/2}$ versus ν can be fitted and the non-linearity due to the third term in eqn. (15) gives the value of k_{off}. From the sodium ion data k_{off} was found to be 3×10^5/s (33-35). This is the off-rate at low concentrations due to the singly occupied state of the channel and is designated k^t_{off}. Thus when the off-rate constant is so slow that the broad component is not observed, it might be determinable in a standard type of line shape analysis (43,44). For the ^{23}Na data the upper limit for a determinable rate constant by this means is about 10^6/s.

B. Interpretation of Ion Correlation Times as Ion Occupancy Times

There are a number of possible contributions to the ion correlation times, that is, of possible sources of fluctuating electric field gradient. These are: τ_r, the reorientation correlation time; τ_{vib}, vibrations

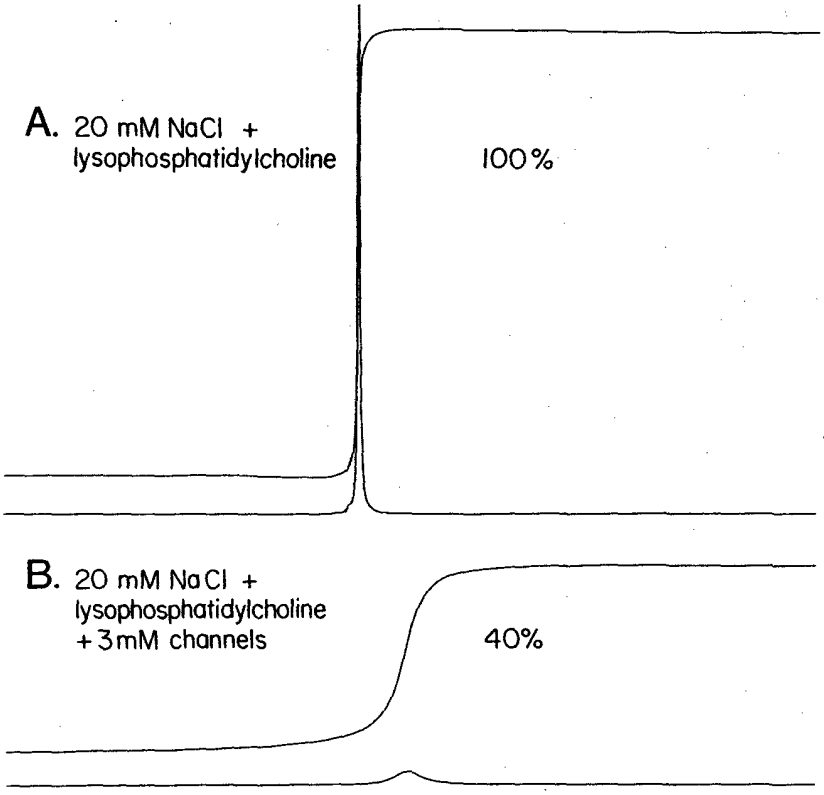

Figure 13. Integration of 20 mM NaCl in the presence of the lipid, lysophosphotidylcholine, which is taken as the reference for 100% of resonance intensity, and of 20 mM NaCl in the presence of the same amount of lipid plus 3 mM channels where the resonance intensity has been found to be reduced to 40%. This is diagnostic of *Case 4* in Figure 5. See text for discussion. Reproduced with permission from reference 11.

or oscillations in the ligand field of the ion at its binding site; τ_{cb}, the central barrier correlation time, i.e. the time for jumping from one site to the other within the channel; and τ_b the ion occupancy time for the channel binding site. The relationship is:

$$\frac{1}{\tau_c} = \frac{1}{\tau_r} + \frac{1}{\tau_{vib}} + \frac{1}{\tau_{cb}} + \frac{1}{\tau_b} \qquad (16)$$

τ_r, the reorientation correlation time As the nuclei are oriented with respect to the magnetic field, the rotation of the system containing the binding site with its electric field gradient constitutes a fluctuating electric field gradient as sensed by the spinning nucleus. In the case of gramicidin A channels packaged in lysophosphotidylcholine bilayer membranes with dimensions of several tens of nanometers (45), the reorientation correlation time would be the order of 10^6/s (46). Since the ion correlation times measured above for the alkali metal ion interactions with the gramicidin A channel are all some two orders of magnitude shorter, τ_r^{-1} would not contribute significantly to τ_c^{-1}

τ_{vib}, vibrations of the ligand field. One means of addressing this possible source of fluctuating electric field gradient is to examine the temperature dependence of τ_c and to determine whether the thermodynamic properties could be those of a vibrational process. The temperature dependence of τ_c is plotted in Figure 14 (7) as $-\ln\tau_c$ versus $T^{-1}(°K)$. Using Eyring rate theory formalism, the slope gives a $\Delta H^{\ddagger}$ of 5.9 kcal/mole and from the value at 303 K $\Delta S^{\ddagger}$ is found to be -5.4 cal/mole·deg. Now for a vibrational process the statistical mechanical expression for entropy using a harmonic oscillator partition function is written,

$$S_i = R\, ln(1 - e^{-h\nu_i/kT})^{-1} + \frac{Nh\nu_i}{T}(e^{h\nu_i/kT} - 1)^{-1} \qquad (17)$$

A vibrational frequency that would have an entropy of 5.4 cal/mole.deg would have a correlation time

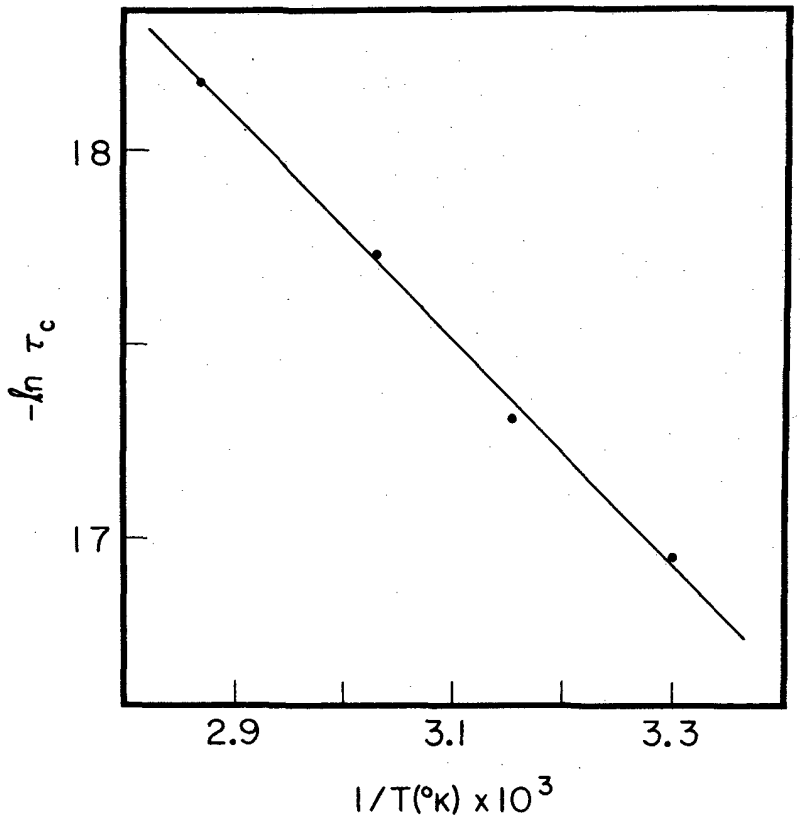

Figure 14. Temperature dependence of $-\ln\tau_c$ plotted versus T^{-1} (°K) for 1 M NaCl in the presence of 3 mM channels. The data results in a linear plot indicating a $\Delta H^{\ddagger}$ of 5.9 kcal/mole and a $\Delta S^{\ddagger}$ evaluated at 303 K using Eyring rate theory, of –5.4 cal/mole·deg. These values are inconsistent with ligand field vibration as a source of fluctuating electric field gradient but are consistent with an energy barrier for channel transport. See text for discussion. Reproduced with permission from reference 7.

$\tau_{vib} = (2\pi\nu_i)^{-1}$ of tenths of a picosecond. As the quantities obtained for the alkali metal ions are in the range of nanoseconds, it is argued that fluctuations of the ion ligands are not the source of the nuclear spin relaxation. Also the enthalpy for a vibrational process would be more than an order of magnitude smaller than 5.9 kcal/mole. The latter is more appropriate to the magnitude of a reaction barrier for a fast process, for example, for a flow of 10^7 ions/s.

τ_{cb}, central barrier correlation time. A jumping of the ion within the channel from one binding site to another could provide a fluctuating electric field gradient because an ion at the head to head junction could experience a different electric field gradient than an ion at a binding site. By this mechanism an ion could experience a fluctuating electric field gradient with a correlation time for an ion passing over the central barrier. This possible contribution can be addressed by considering two channels which differ primarily in the rate at which the ions pass over the central barrier. The two channels are the gramicidin A channel and the malonyl gramicidin A channel. In the latter case the formyl moieties are removed from gramicidin A and two molecules are tied together by the malonyl moiety, CO-CH_2-CO. The single channel currents of the malonyl GA channel are smaller than for the GA channel. Also from dielectric relaxation studies the rate for thallium ion passage over the central barrier, k_{cb} is 4×10^6/s for the malonyl GA channel (47) whereas it is greater than 5×10^7/s for the GA channel (48). These values differ by more than an order of magnitude, yet for sodium ion the value of τ_c is 48 ns in

both cases (7,33-35). This indicates that the jump over the central barrier, i.e. the ion translocation between the sites within the channel, is not affecting τ_c.

τ_b, the ion occupany time. When the rate at which the ion exchanges between site and solution is faster than the relaxation rate at the site, i.e. R_{1b}, the process of entering and leaving the channel constitutes a fluctuation in the electric field gradient experienced by the ion. The characteristic time for the process would be the ion occupancy time, and the inverse of the ion occupancy time would be the off-rate constant, $\tau_b^{-1} = k_{off}$. By the process of elimination above, it has been deduced that τ_c for this system is actually τ_b, that is,

$$\tau_c^{-1} \simeq k_{off} \tag{18}$$

for the alkali metal ion interactions with the Gramicidin A transmembrane channel.

The rate constants, therefore, obtained for the alkali metal ions are summarized in Table III.

V. Calculation of Gramicidin A Single Channel Currents Using NMR Derived Binding and Rate Constants

It is possible with only the weak binding constant, K_b^w, and the weak off-rate constant, k_{off}^w to obtain quite reasonable values for the single channel currents and for the conductance ratios. This is the case directly for ^{23}Na, ^{39}K and ^{87}Rb. It is also the case for ^{133}Cs assuming that the two phenomenological components in the transverse relaxation of this spin 7/2 nucleus can be treated as a spin 3/2 nucleus. And we have noted above that inclusion of the dipole-dipole relaxation mechanism with the quadrupolar relaxation mechanism would give reasonable lithium-hydrogen internuclear distances with a correlation time capable of calculating the experimental currents. Also it is possible to calculate the single channel currents at a given applied potential over large ion activity ranges, e.g. from 10 mM activity to several molal activity. This requires NMR-derived estimates of K_b^w, k_{off}^w, K_b^t and k_{off}^t for all of the alkali metal ions and in addition it requires dielectric relaxation data for the rate of intrachannel ion translocation, i.e. for the rate over the central barrier. This has been done for the sodium ions (23). Here for brevity, however, the high ion activity approximation will be used.

A. Approximate Calculation for High Ion Activities

For sodium ion the off-rate constant for single ion occupancy of the channel, k_{off}^t, is approximated as 3×10^5/s. This would result in too small a flow of ions to be measurable. In this case the first ion in the channel is electrically silent and it is necessary only to consider the probability of the singly occupied state, χ_s, and the probability of the doubly occupied state, χ_d, with $\chi_s + \chi_d = 1$. To a good approximation, when a potential (positive on the entry side) is applied, the entry barrier may be taken as rate limiting. The current, i, over that barrier is written

$$i = forward\ rate\ -\ backward\ rate \tag{19}$$

and

$$i = [Me^+]k_{on}^w\chi_s e^{\ell_f zEF/2dRT} - \chi_d k_{off}^w e^{-\ell_b zFE/2dRT} \tag{20}$$

Writing ϵ_f and ϵ_b for the exponential powers, recognizing that $K_b^w k_{off}^w = k_{on}^w$', and that $\chi_s = 1 + [Me^+]\,K_b^w)^{-1}$ and that $\chi_d = [Me^+]\,K_b^w(1+[Me^+]\,K_b^w)^{-1}$, eqn. (20) becomes

$$i = \frac{[Me^+]K_b^w k_{off}^w}{(1+[Me^+]K_b^w}(e^{\epsilon_f} - e^{\epsilon_b}) \tag{21}$$

At one molal ion activity $[Me^+] = 1$ and the expression is simply

$$i = \frac{K_b^w k_{off}^w}{(1+K_b^w)}(e^{\epsilon_f} - e^{\epsilon_b}) ions/s \tag{22}$$

With the known structure in Figures 2 and 3, the distances between binding site and exit barrier, ℓ_b, and between solution and entry barrier, ℓ_f, are approximately 3Å and the total distance across the channel, 2d, is taken as 30Å. z is the charge on the ion, i.e. one; F is the Faraday (23 kcal/mole·volt); E is the applied potential (0.1 volt); R is the gas constant (1.987 cal/mole·deg); and T is the absolute temperature (303 K) such that the Eyring factor $(e^{\epsilon_f} - e^{\epsilon_b})$ equals 0.78. Thus with the values in Table I for K_b^w and Table III for k_{off}^w, the currents are calculated at one molal ion activity. These values are listed in Table IV. To convert from ions/s to

Table III. Rate Constants for Alkali Metal Ion Interactions with the Gramicidin A Transmembrane Channel.

Ion	k^t_{off}	k^w_{off}	Reference
$^7Li^+$		4.5×10^7/s $(0.85 \times 10^7$/s)[a]	(11)
$^{23}Na^+$	3×10^5/s (~50mM NaCl)	2.1×10^7/s	(7,33,35)
$^{39}K^+$		2.6×10^7/s	(10)
$^{87}Rb^+$		7.4×10^7/s	(8,11)
$^{133}Cs^+$	1.4×10^7/s (30mM CsCl)	5.9×10^7/s (>1.5M CsCl)	(11,12)

[a]Obtained on introduction of the dipole-dipole relaxation mechanism for ^{7}Li with the τ_c chosen to give the correct off-rate constant (see eqn.18). The test for this is whether the value obtained for Li–H internuclear distances for the ion in the channel is reasonable. The value is equivalent to four hydrogen atoms each at 2.4 Å from the lithium nucleus. This is not an unreasonable value.

Table IV. Approximate Calculation of Single Channel Currents and Conductances.

Ion	Single channel[a] current i(ions/s)	Single channel[b] conductances γ (pS)	Conductance Ratios γ(Me)/γ(Na)[c]	
			calc'd	expt'l
Li^+	0.29×10^{7d}	4.6	0.25	0.24
Na^+	1.18×10^7	19	1	1
K^+	1.81×10^7	29	1.5	~2
Rb^+	4.59×10^7	73	3.9	>3
Cs^+	3.72×10^7	56	3.2	>3

[a]The single channel current at one molal activity is given by eqn. (22); $i = 0.78\ K^w_b k^w_{off}\ /(1 + K^w_b)$ ions/s.
[b]The single channel conductance, $\gamma = i \times 1.6 \times 10^{19}$ ampere/0.1 volt.
[c]The conductance ratios vary with lipid and with ion activity. The ratios with respect to that of sodium ion for Rb^+ and Cs^+ are generally slightly greater than 3 with that for Rb^+ being about 10% greater than that for Cs^+.
[d]Single channel current for Li^+ was obtained using a value for τ_c that had been chosen on addition of the dipole-dipole relaxation mechanism to give a correct current. The test as to the appropriateness of the value is the reasonableness of the Li–H internuclear distances necessary for that τ_c. The value for the sum over distances (see eqn.12) is not unreasonable.

coulombs/s or amperes, the value for ions/s is multiplied by 1.6×10^{-19} coulombs/ion. On division of the current in amperes by the applied potential, 0.1 volt, the conductance, γ, is obtained in Siemens (Ω^{-1}). The values are usually given as picosiemens (pS). These values are also given in Table IV as are the calculated conductance ratios given with respect to the conductance of the sodium ion γ(Na).

The electrically measured most probable single channel conductances have been determined using diphytanoyl phosphatidylcholine/n-decane membranes at 100 mV and 30° for 1 M KCl (0.605 molal activity) to be 26 pS (49) and for 1 M CsCl (0.544 molal activity) to be 48 pS (29). The calculated sin-

gle channel conductances using eqn.(21) are 27 pS for potassium ion and 51 pS for cesium ion. The calculated single channel conductance for KCl is within 4% of the experimental value and that for CsCl is within 6% of the experimental measurement of this conductance. The calculated single channel conductance ratios are also remarkably close to the experimental conductance ratios (2-4,13,14) as listed in Table IV. These results provide a sound basis for utilizing NMR relaxation studies to determine binding and rate constants relative to channel transport processes when single channel currents are in the range of $10^{6.5}$ to 10^{8} ions/s.

Acknowledgement: The author gratefully acknowledges past and present members of the Laboratory of Molecular Biophysics, who have contributed so significantly to work reviewed here. This work was supported in part by NIH grant GM 26898.

VI. REFERENCES

[1]E. Bamberg and P. Läuger, *Biochim. Biophys. Acta* **367**, 127 (1974).

[2]S. B. Hladky and D. A. Haydon, *Current Topics in Membranes and Transport* **21**, 327, (1984).

[3]E. Bamberg, K. Noda, E. Gross, and P. Laüger, Biochim. Biophys. Acta 223 (1976).

[4]G. Eisenman, J. Sandblom, and E. Neher, *Biophys. J.* **22**, 307 (1978).

[5]0. S. Anderson, *Biophys. J.* **41**, 119 (1983).

[6]B. Sakmann and E. Neher in *Single-Channel Recording*, Plenum Publishing Company, New York, 1983.

[7]D. W. Urry, T. L. Trapane, C. M. Venkatachalam and K. U. Prasad, *Int. J. Quantum Chem.: Quantum Biol. Symp.* **12**, 1-13 (1986).

[8]D. W. Urry, T. L. Trapane, C. M. Venkatachalam and K. U. Prasad, J. Am. Chem. Soc. **108**, 1448-54 (1986).

[9]S. Forsén and B. Lindman, in *Methods of Biochemical Analysis*, D. Glick, Ed., John Wiley and Sons, New York, 1981, p. 289.

[10]D. W. Urry, T. L. Trapane, and C. M. Venkatachalam, *J. Membr. Biol.* **89**, 107-111 (1986).

[11]D. W. Urry, T. L. Trapane, C. M. Venkatachalam, and R. B. McMichens, in *Biomembranes Biological Transport Volumes of Methods in Enzymology*, Sidney Fleischer, Ed., Academic Press, Inc., New York, New York (in press).

[12]D. W. Urry and T. L. Trapane, *J. Magn. Reson.* **71**, 193-200 (1987).

[13]S. B. Hladky and D. A. Haydon, *Biochim. Biophys. Acta* **274**, 294-312 (1972).

[14]V. Myers and D. A. Haydon, *Biochim. Biophys. Acta* **274**, 313 (1976).

[15]P. Mueller and D. 0. Rudin, *Biochim. Biophys. Res. Commun.* **26**, 398 (1967).

[16]D. W. Urry, S. Alonso-Romanowski, C. M. Venkatachalam, T. L. Trapane and K. U. Prasad, *Biophys. J.* **46**, 259-265 (1984).

[17]C. M. Venkatachalam, S. Alonso-Romanowski, K. U. Prasad and D. W. Urry, *Int. J. Quantum Chem.: Quantum Biol. Symp.* **11**, 315-326 (1984).

[18]D. W. Urry, *Proc. Natl. Acad. Sci. USA* **68**, 672-676 (1971).

[19]D. W. Urry, M. C. Goodall, J. D. Glickson and D. F. Mayers, *Proc. Natl. Acad. Sci. USA* **68**, 1907-1911 (1971).

[20]D. W. Urry, in *The Enzymes of Biological Membranes*, A. N. Martonosi, Ed., Plenum Publishing Corporation, New York, New York, 1985, pp. 229-257.

[21]R. Sarges and B. Witkop, *J. Am. Chem. Soc.* **87**, 2011-2020 (1965).

[22]R. Sarges and B. Witkop, *J. Am. Chem. Soc.* **87**, 2020-2027 (1965).

[23]D. W. Urry, in *Topics in Current Chemistry*, F. L. Boschke, Ed., Springer-Verlag, Heidelberg, Germany, **128**, 1985, pp. 175-218.

[24]D. W. Urry, T. L. Trapane and K. U. Prasad, *Science* **221**, 1064-1067 (1983).

[25]D. W. Urry, J. T. Walker and T. L. Trapane, *J. Membr. Biol.* **69**, 225-231 (1982).

[26]I. Pasquali-Ronchetti, A. Spisni, E. Casali, L. Masotti and D. W. Urry, *Bioscience Reports* **3**, 127-133 (1983).

[27]T. L. James and J. H. Noggle, *Proc. Nat. Acad. Sci. USA* **62**, 644 (1969).

[28]T. E. Bull, S. Forsén, and D. L. Turner, *J. Chem. Phys.* **70**, 3106 (1979).

[29]D. W. Urry, T. L. Trapane, R. A. Brown, C. M. Venkatachalam and K. U. Prasad, *J. Magn. Reson.* **65**, 43-61 (1985).

[30]D. W. Urry, T. L. Trapane, C. M. Venkatachalam and K. U. Prasad, *J. Phys. Chem.* **87**, 2918-2923 (1983).

[31]T. E. Bull, *J. Magn. Reson.* **8**, 344 (1972).

[32]K. Rose and R. G. Bryant, *J. Magn. Reson.* **31**, 41 (1978).

[33]D. W. Urry, C. M. Venkatachalam, A. Spisni, P. Läuger and M. A. Khaled, *Proc. Natl. Acad. Sci., USA* **77**, 2028-2032 (1980).

[34]C. M. Venkatachalam and D. W. Urry, *J. Magn. Reson.* **41**, 313-335 (1980).

[35]D. W. Urry, C. M. Venkatachalam, A. Spisni, R. J. Bradley, T. L. Trapane and K. U. Prasad, *J. Membr. Biol.* **55**, 29-51 (1980).

[36]P. C. Schmidt, K. D. Sen, T. P. Das and A. Weiss, *Phys. Rev. B.* **22**, 4167-4179 1980.

[37]P. Lazlo, in *The Multinuclear Approach to NMR Spectroscopy*, J. B. Lambert and F. G. Riddell, Editors, D. Reidel Publishing Company, Boston, 1980, pp. 261-296.

[38]E. Göbel, W. Müller-Warmuth and H. Olyschläger, *J. Magn. Reson.* **36**, 371-87 (1979).

[39]E. T. Fossel, M. M. Sarasua and K. A. Koehler, *J. Magn. Reson.* **64**, 536-540 (1985).

[40]F. W. Wehrli, *J. Magn. Reson.* **23**, 527-532 (1976).

[41]A. Allerhand, D. Doddrell R. Komoroski, *J. Chem. Phys.* **55**, 189-198 (1971).

[42]I. Solomon, *Phys. Rev.* **99**, 559-565 (1955).

[43]G. Binsch, in *Topics in Stereochemistry*, E. L. Eliel and N. L. Allinger Eds., Wiley, New York, 1968, p. 97.

[44]J. Feeney, J. G. Batchelor, J. P. Albrand, G. C. K. Roberts, *J. Magn. Reson.* **33**, 519 (1979).

[45]A. Spisni, I. Pasquali-Ronchetti, E. Casali, L. Lindner, P. Cavatorta, L. Masotti and D. W. Urry, *Biochim. Biophys. Acta* **732**, 58-68, (1983).

[46]A. F. Horwitz, W. J. Horsley and M. . Klein, *Proc. Nat. Acad. Sci. USA* **69**, 590-593 (1972).

[47]R. Henze, E. Neher, T. L. Trapane and D. W. Urry, *J. Membr. Biol.* **64**, 233-239 (1982).

[48]R. Henze and D. W. Urry, unpublished data.

[49]D. W. Urry, S. Alonso-Romanowski, C. M. Venkatachalam, R. J. Bradley and R. D. Harris, *J. Memb. Biol.* **81**, 205-217 (1984).